IEEE Access
Multidisciplinary | Rapid Review | Open Access Journal

Received November 11, 2019, accepted December 12, 2019, date of publication December 18, 2019,
date of current version December 27, 2019.

Digital Object Identifier 10.1109/ACCESS.2019.2960512

Series Arc Fault Detection of Indoor Power Distribution System Based on LVQ-NN and PSO-SVM

NA QU[1,2], JIANKAI ZUO[3], JIATONG CHEN[4], AND ZHONGZHI LI[3]
[1]School of Safety Engineering, Shenyang Aerospace University, Shenyang 110136, China
[2]Liaoning Key Laboratory of Aircraft Safety Airworthiness, Shenyang Aerospace University, Shenyang 110136, China
[3]School of Computer Science, Shenyang Aerospace University, Shenyang 110136, China
[4]School of Aviation Engine, Shenyang Aerospace University, Shenyang 110136, China

Corresponding author: Na Qu (mn_qn@qq.com)

This work was supported in part by the National Natural Science Foundation of China under Grant 61901283, and in part by the Department of Education Project of Liaoning Province under Grant L201742.

ABSTRACT When a series arc fault occurs in indoor power distribution system, current value of circuit is often less than the threshold of the circuit breaker, but the temperature of arc combustion can be as high as thousands of degrees, which can lead to electrical fire. The arc fault experimental platform is used to collect circuit current data of normal work and arc fault. Five types of loads which are commonly used in indoor distribution system, such as resistive and inductive in series load, resistive load, series motor load, switching power load and eddy current load, are chosen. This paper uses four features of current in time domain, *i.e.* current average, current pole difference, difference current average and current variance. Ten features of current in frequency domain are extracted by Fast Fourier Transform (FFT). The learning vector quantization neural network (LVQ-NN) is designed to judge the load type. The support vector machine optimized by particle swarm optimization (PSO-SVM) is designed to detect the arc fault. The simulation results show the effectiveness of the proposed method.

INDEX TERMS Arc fault, LVQ-NN, PSO-SVM, indoor power system.

I. INTRODUCTION

With the continuous increase of high-rise buildings, the scale and capacity of indoor power distribution systems are also rapidly expanding and the risk of electrical fires is also increasing. Electrical fire generally refers to that high temperature, arcing and so on caused by electrical line and equipment faults lead to ignite themselves or other combustible materials. According to the analysis of relevant data, the series arc fault of the power distribution system has become one of the main causes of electrical fires.

Arc fault detection research mainly focuses on arc simulation model, current feature extraction and detection algorithm. Studying these arc model is useful for understanding the physical nature of arc and play an active role in detecting arc fault. Cassie and Mayr model are proposed early [1], [2].

The associate editor coordinating the review of this manuscript and approving it for publication was Francesco Tedesco.

The equation of Cassie model is

$$\frac{1}{g}\frac{dg}{dt} = \frac{d\ln g}{dt} = \frac{1}{\tau}\left(\frac{u^2}{U_C^2} - 1\right) \tag{1}$$

where g is the conductance of the arc, u is the voltage across the arc, τ is the arc time constant, U_c is the constant arc voltage.

The equation of Mayr model is

$$\frac{1}{g}\frac{dg}{dt} = \frac{d\ln g}{dt} = \frac{1}{\tau}\left(\frac{ui}{P} - 1\right) \tag{2}$$

where g is the conductance of the arc, u is the voltage across the arc, i is the arc current, τ is the arc time constant.

Cassie model is mainly suitable for large current period before zero crossing. Mayr model is mainly suitable for small current period when zero crossing. On the basis of Cassie model and Mayr model, Habedank model [3], modified Mayr model [4], Schwamaker model [5], segmented arc model [6]–[9] and so on, have been proposed.

The main methods of current feature extraction are Fast Fourier transform (FFT) [10], [11], wavelet transform (WT) [12]–[16] and Chirp-zeta transform (CZT) [17]. FFT is used to get the current amplitude spectrum and the arc fault detection is based on the different distribution characteristics of normal work and arc fault. WT mainly uses discrete multi-scale wavelet to decompose current signals, and chooses appropriate wavelet coefficients as detection features of arc fault. CZT allows to perform spectral analysis in a smaller frequency band compared with FFT. A few load types (such as electric hand-held dill in minimum speed) are not suitable for arc fault detection by CZT method.

The arc fault detection algorithms mainly include BP neural network [18], support vector machine (SVM) [19], [20], matrix coefficients [21], and quantum probability mode [22] etc. BP neural network and SVM are often used in indoor power distribution system. The matrix coefficients method is to establish the relationship between input current and output current through a transfer matrix. The matrix coefficients depend on conductor parameters, arc fault and load types. This method is mainly applied to aircraft arc fault detection because aircraft supply environment have fewer load types.

Aircraft electric wire can be modeled as a transmission line with the resistance, inductance, shunt capacitance, and shunt conductance. In indoor power distribution system, there are many load types, so it is not suitable to use matrix coefficients method to detect arc fault. The quantum probability model is mainly applied to the photovoltaic power system. Based on the calculated entropy, the model is able to differentiate an arc state from a no-arc state. The model enables arc fault detection on a plug-and-play principle, requiring no prior information about the PV system in which it operates.

This paper takes the series arc fault of indoor power distribution system as the research object and studies the influence of arc fault on the circuit current under different types of load conditions. The current features of time and frequency domain are extracted respectively and they have different characteristics in normal work and arc fault state. The novel load type and arc fault detection methods are presented and its effectiveness is shown in several load conditions.

Learning vector quantization neural network (LVQ-NN) is used to judge the load type. SVM optimized by particle swarm optimization (PSO-SVM) is used to detect the arc fault. Compared with conventional SVM and BP neural network, PSO-SVM can detect arc fault faster and more accurately.

This paper is organized as follows. Section II provides acquisition experiment of arc fault current under different loads conditions. Section III provides features extraction of time domain and frequency domain. In section IV, LVQ-NN is used to judge the load type and PSO-SVM algorithm is designed to identify normal work or arc fault. The block diagram of complete description is shown as Figure 1.

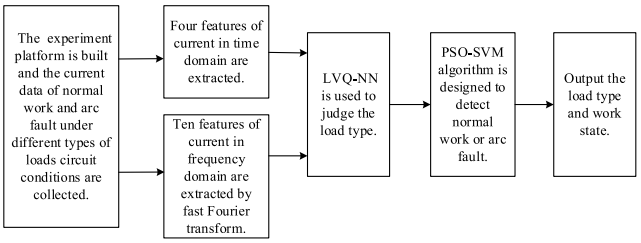

FIGURE 1. The block diagram of complete description.

II. SERIES ARC FAULT EXPERIMENT

According to the international standard UL1699, the experimental platform for arc fault is used to collect circuit current data of normal work and arc fault, the load types and corresponding sampling resistance, as shown in Figure 2 [23]. The arc generator is mainly composed of a fixed carbon electrode, a moving copper electrode, an insulating block, an insulating clip, a lateral adjusting device and a fixed insulating base. TDS1001C-SC of Tektronix oscilloscope and TPP0101 10X of voltage probe are selected to complete the experiment. The loads are that commonly used in indoor power distribution system, such as resistive and inductive in series load, resistive load, series motor load, eddy current load and switching power load. The current waveform is obtained by the sampling resistance method. The current waveform is shown in Figure 3-7. The sampling resistance is 100 ohms when the loads are resistive load, resistive and inductive load. The unit of ordinate is 0.01A in Figure 3 and Figure 4. The sampling resistance is 50 ohms when the loads are series motor load and switching power load. The unit of ordinate is 0.02A in Figure 5 and Figure 6. The sampling resistance is 1 ohm when the load is eddy current load. The unit of ordinate is 1A in Figure 7.

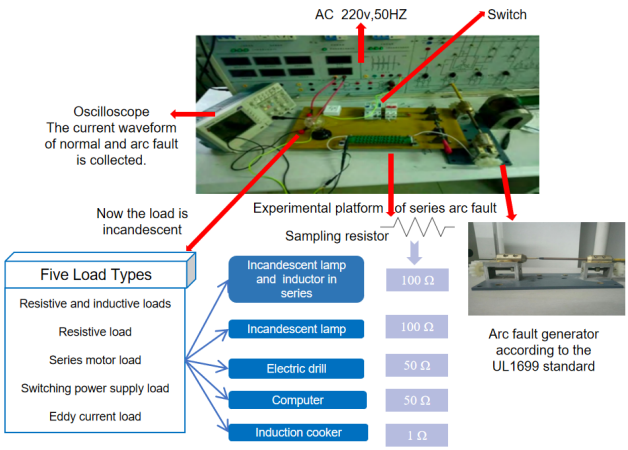

FIGURE 2. Schematic diagram of arc fault experiment.

III. FEATURE EXTRACTION

The circuit current data of different loads under normal work and arc fault conditions are recorded. In order to detect arc

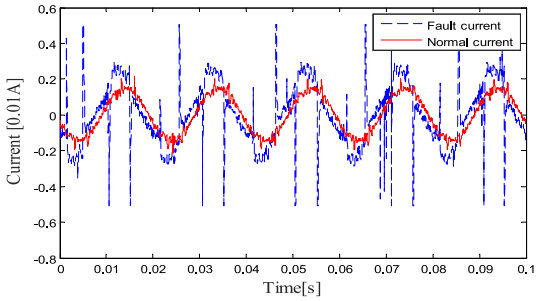

FIGURE 3. Current waveform of incandescent lamp and inductor in series.

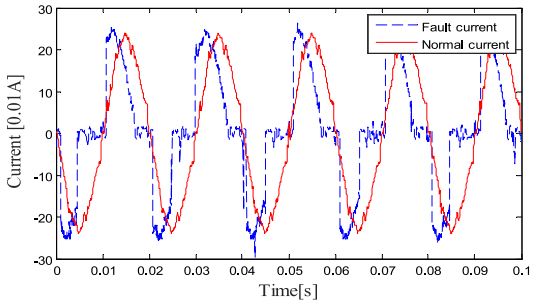

FIGURE 4. Current waveform of incandescent lamp.

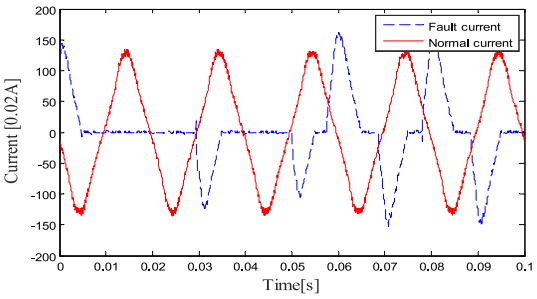

FIGURE 5. Current waveform of electric drill.

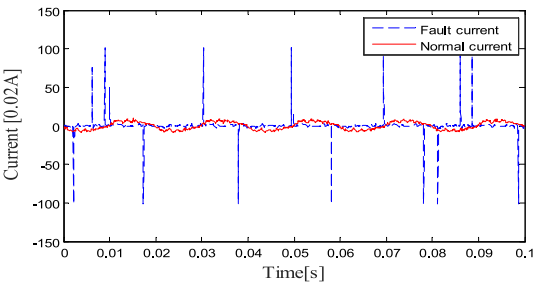

FIGURE 6. Current waveform of computer.

fault accurately, the current features are extracted from both time domain and frequency domain.

A. TIME DOMAIN FEATURE EXTRACTION

In the time domain, one cycle of current data is divided into ten equal-length time segments. Ten segments of a cycle not only reflect the main information of original data, but also avoid a large amount of computation and ensure the

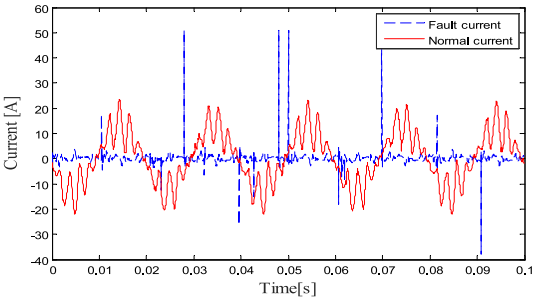

FIGURE 7. Current waveform of induction cooker.

real-time performance. In order to enable each data point to express the same information, each segment is equal in length. Four features of current in time domain, *i.e.* current average, current pole difference, difference current average and current variance, are extracted. The current average, current pole difference and current variance respectively correspond to one number in each segment and ten numbers in one cycle. The difference average contains nine numbers in one cycle, because it is obtained by calculating the current difference between two adjacent segments. Thirty-nine numbers is extracted as feature values of current in time domain.

1) CURRENT AVERAGE

The current average is the average value of current in each segment time, as shown in (3). This feature can represent the overall distribution of current value in time domain and reduce the influence of individual abnormal current value (such as too large or too small current value at a point).

$$I_{ave} = \frac{1}{n}\sum_{i=1}^{n} I_i \tag{3}$$

where n is the number of current value in one segment, I_i is the i^{th} current value in a time segment. The sampling interval is 4×10^{-4}s and AC frequency is 50 Hz (a cycle is 0.02s), then 50 current values can be measured in one cycle. One cycle is divided into 10 segments, and the corresponding 50 current values are also divided into 10 groups. So there are 5 numbers in each segment, *i.e.* n is 5.

2) CURRENT POLE DIFFERENCE

The current pole difference is the difference between maximum and minimum of current in one segment, as shown in (4). This feature can reflect the change of current value in a time segment.

$$I_{ran} = I_{\max} - I_{\min} \tag{4}$$

$I_{\max}$ is the maximum of current in one segment, $I_{\min}$ is the minimum of current in one segment.

3) DIFFERENCE AVERAGE

Difference average is the average of difference between the corresponding current values in adjacent segments, as shown

in (5). This feature can reflect the change of current value in adjacent two time segments.

$$I_D = \frac{1}{n}\sum_{i=1}^{n}(I_{i+n} - I_i) \tag{5}$$

I_i represents the i^{th} current value in the segment, I_{i+n} represents that the current value of the corresponding position in the next segment.

4) CURRENT VARIANCE

The current variance is the variance of current in one segment, as shown in (6). This feature represents the dispersion of current amplitude in each time segment.

$$I_{var} = var(I_1, \quad I_2, \cdots I_n) \tag{6}$$

where $var(\ )$ represents the variance of a set of data. $I_1, I_2, \ldots, I_n$ represents all current values in one segment.

Here, the current features of incandescent lamp load circuit is taken as an example, as shown in Figure 8. It can be seen that the values of four features under normal work and arc fault are obviously different and these four features can be used to distinguish arc fault from normal work.

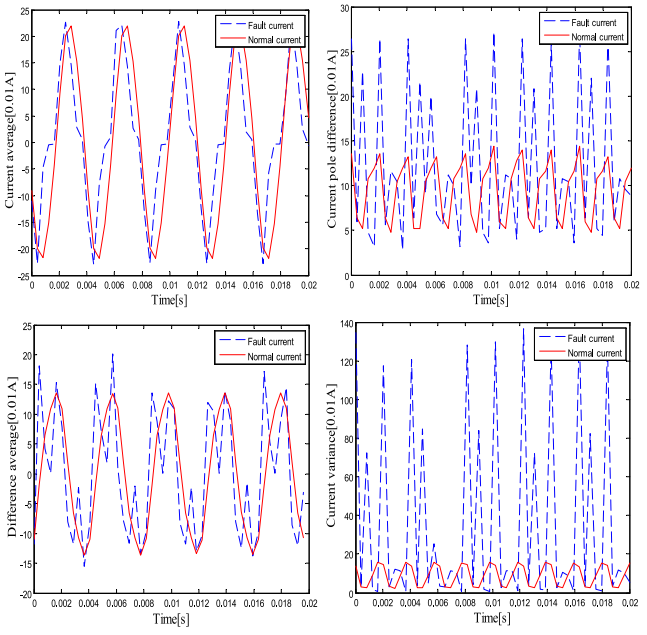

FIGURE 8. Feature extraction of incandescent lamp load circuit in time domain. (a) Current average. (b) Current pole difference. (c) Difference average. (d) Current variance.

B. FREQUENCY DOMAIN FEATURE EXTRACTION

The fast Fourier transform (FFT) is used to extract features of current in frequency domain [24]. The frequency range is 0∼2000Hz and divided into ten intervals. Each interval is 200Hz. According to 50Hz frequency of AC, four amplitudes are extracted by FFT every interval. The average of four amplitudes is taken as the interval feature in order to reduce the computations. In total, there are ten feature values in the frequency domain. The connection of ten feature values under normal work and arc fault conditions is drawn, as Figure 9. In the low frequency band, the current amplitude of arc fault is higher than that of normal work when the loads are incandescent lamp and inductor in series, incandescent lamp and electric drill. The current amplitude of arc fault is lower than that of normal work when the loads are computer and induction cooker. In the high frequency band, the current amplitude of arc fault is higher than that of normal work in all loads circuits. The conclusion is that the current of arc fault contains more harmonic wave.

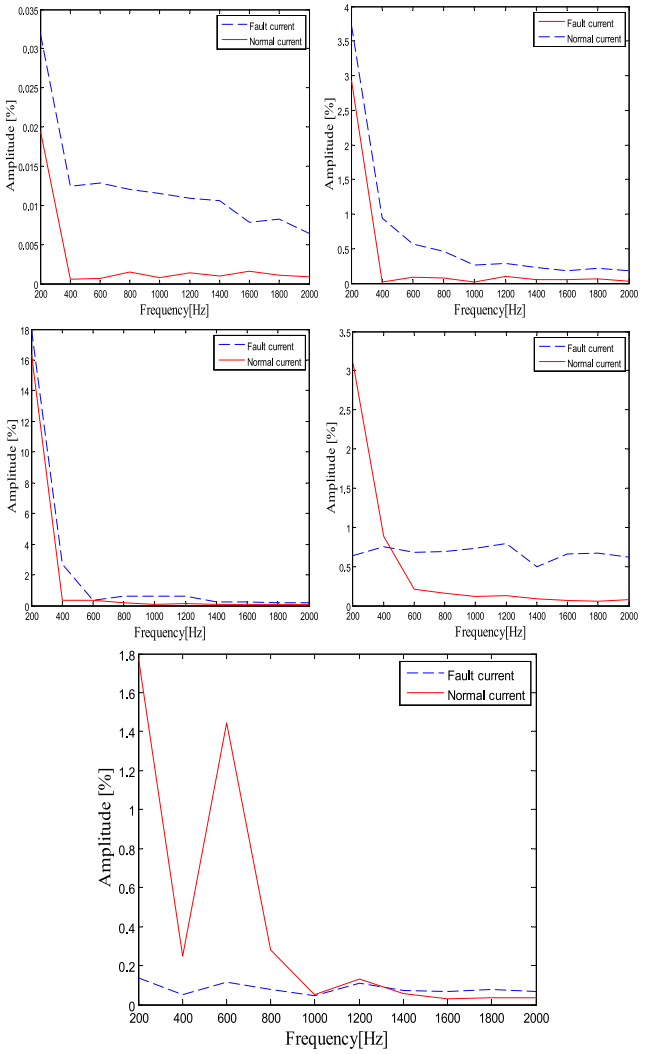

FIGURE 9. Feature extraction in frequency domain. (a) Incandescent lamp and inductor in series load. (b) Incandescent lamp load. (c) Electric drill load. (d) Computer load. (e) Induction cooker load.

IV. LOAD CLASSIFICATION AND ARC FAULT DETECTION

According to different types of load circuits have different current features, LVQ-NN is used to judge the load type and PSO-SVM algorithm is designed to detect arc fault.

A. LOAD CLASSIFICATION BASED ON LVQ-NN

The LVQ-NN which proposed on the basis of competitive neural network is a supervised learning network with the advantages of simple structure, strong adaptive ability and strong classification ability [25]. The structure of the LVQ-NN is suitable for multi-classification problems and shown in Figure 10. There are five types of loads and all samples are divided into five types, which belongs to the multi-classification problem.

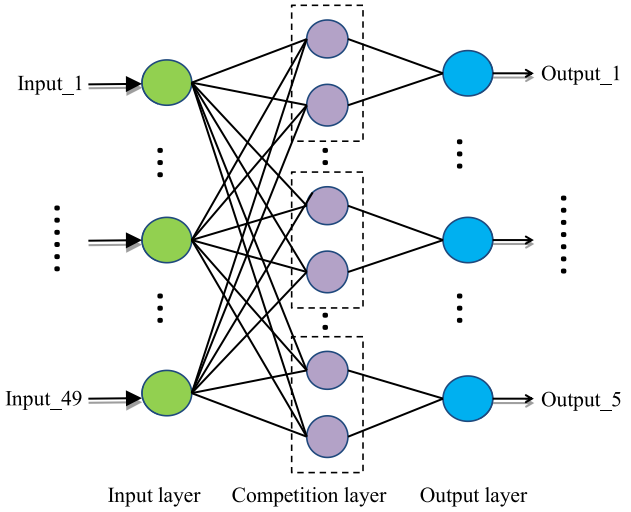

FIGURE 10. LVQ-NN topology structure.

The main steps of LVQ-NN algorithm are as follows.

(a) Initialize the connection weight between the competition layer and the input layer, and other network parameters.

(b) Calculate the Euclidean distance of weight vector corresponding to all the competitive layer neurons and the input vector, as (7).

$$L = \sqrt{\sum_{i=1}^{m} (x_i - w_{ij})^2} \tag{7}$$

where x_i represents the input vector and w_{ij} represents the connection weight of the competing neuron.

(c) If the category of output layer neuron corresponding to the nearest neuron is the same as actual category of data, the weight of the competing neuron is modified according to (8).

$$w_{new} = w_{old} + \eta(x - w_{old}) \tag{8}$$

Otherwise, the weight of the competing neuron is modified according to (9).

$$w_{new} = w_{old} - \eta(x - w_{old}) \tag{9}$$

where w_{new} and w_{old} respectively represent the corrected weight and the weight before correction, η represents the learning rate.

The category labels 1, 2, . . . , 5 are used to indicate the five types of loads, such as incandescent lamp and inductor in series, incandescent lamp, induction cooker, computer and hand drill. The feature values of current in time domain and frequency domain are selected as LVQ-NN inputs. The number of features in time domain is thirty-nine and that in frequency domain is ten.

In total, the number of features is forty-nine and the number of network input layer nodes is forty-nine. The number of output layer nodes is five which is equal to the number of load types. After simulation trainings, the optimal number of competitive layer nodes is determined to be fifty. The learning rate is set to 0.05, the target error is set to 0.08 and the maximum number of training steps is set to 200.

TABLE 1. Load classification results of LVQ-NN and BP network.

Load	Samples number	Correct number		Correct rate	
		LVQ	BP	LVQ	BP
Incandescent lamp and inductor in series	40	40	5	100%	12.5%
Incandescent lamp	40	40	7	100%	17.5%
Electric drill	40	39	37	97.5%	92.5%
Computer	40	38	4	95%	10%
Induction cooker	40	38	39	95%	97.5%
Total	200	195	92	97.5%	46%

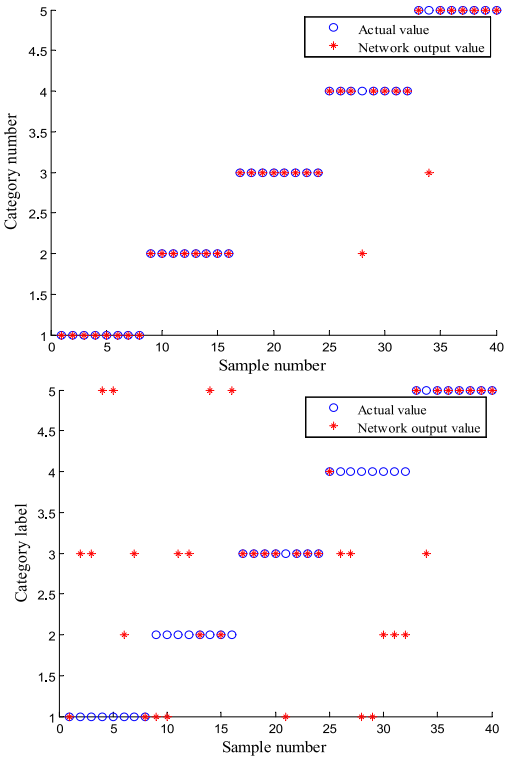

FIGURE 11. Load classification results. (a) LVQ-NN model. (b) BP network model.

Load classification results of LVQ-NN and BP network are shown in Table 1 and Figure 11. Training process of LVQ-NN is shown in Figure 12. In Figure 11, the horizontal

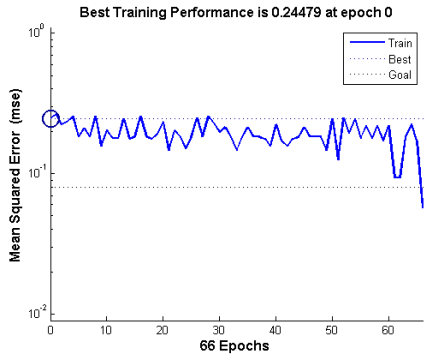

FIGURE 12. LVQ-NN training process.

axis represents the sample number, and the vertical axis represents the load type number. Eight groups of data for each load type are selected as representatives, and a total of forty groups of data are displayed. In the same type of sample, the blue circle indicates the correct category and the red asterisk indicates the category of network output. If the two symbols coincide, the classification result is right. Otherwise, the classification result is wrong. In Figure 12, the horizontal axis represents training times, and the vertical axis represents the mean square error. The network achieves the target error after 66 times. The accuracy of the LVQ-NN model is 100% when the loads are incandescent lamp and inductor in series, incandescent lamp. The accuracy of the LVQ-NN model is 95% when the load is computer and induction cooker. In total, the classification accuracy of LVQ-NN is 97.5%, higher than that of BP network.

B. ARC FAULT DETECTION BASED ON PSO-SVM

SVM arising from statistical learning theory and structural risk minimization (SRM) principles is a machine learning algorithm of supervised classification [26], [27]. SVM can avoid falling into the local minimum value and shows better classification performance in the case of small and high dimension nonlinear samples, in contrast to neural-network based methods. SVM is usually designed as a binary classifier in order to find an optimal hyperplane that can correctly distinguish positive and negative samples. When the samples are linearly inseparable, the concept of "soft interval" is introduced, that is to say, a small number of outliers are allowed, and relaxation variable $\xi i > 0$ is often added. At the same time, a penalty factor c is needed, which represents the tolerance of outliers. It is one of the important parameters affecting the classification performance of SVM, as (10).

$$\min \frac{1}{2}\|\vec{\omega}\|^2 + c\sum_{i=1}^{n} \xi_i$$
$$y_i(\vec{\omega}^T \vec{x}_i + b) \geq 1 - \xi_i \quad i = 1, 2 \cdots, n \tag{10}$$

where (x_i, y_i) represents the i^{th} set of samples, ω represents the normal vector of the hyperplane, n represents the sample size, b is the coefficient in the hyperplane equation, c is the penalty parameter; ξi is the relaxation factor.

In order to transform the linear non-separable samples in low-dimensional space into linear separable samples in high-dimensional space, it is necessary to establish a mapping relationship from low-dimensional space to high-dimensional space. At the same time, in order to simplify the calculation, the kernel function is introduced. The commonly kernel functions include linear, polynomial and radial basis function (RBF). RBF can map features to high-dimensional space and has less computation, as (11).

$$K(x_1, x_2) = e^{-g\|x_1 - x_2\|^2} \tag{11}$$

where g is the kernel parameter, which represents the width of the function. Therefore, the classification performance of SVM greatly depends on appropriate selection of c and g.

When the parameters c and g are selected, the conventional method is that the values of c and g are taken respectively with a certain step and range. The K cross-validation (K-CV) method is used to calculate the classification accuracy. The sample set is divided into K groups, and each group of sample is used as testing set once. The rest of data is used as training set. The average of K accuracy rates is taken as the final classification accuracy. The optimal parameters are selected according to the best final accuracy. However, this method has a large amount of calculations and time-consuming. The improper selection of parameters may lead to the unsatisfactory classification result of SVM.

In order to improve the calculation speed and classification accuracy, PSO algorithm is used to optimize c and g. PSO is a swarm intelligence optimization algorithm and the purpose is to solve the optimal value by imitating the movement rule of birds in the process of predation. The main training process of the PSO algorithm is as follows.

(a) Determine the fitness function and generate a certain number of particles in the feasible domain. Each particle is a potential optimal solution.

(b) Calculate the each particle value according to the fitness function, and select the individual and group extremum. Then update the position and velocity of all particles according to (12) and (13).

$$V_{k+1} = \omega V_k + c_1 a_1 (P_i - X) + c_2 a_2 (P_g - X) \tag{12}$$
$$X_{k+1} = X_k + V_{k+1} \tag{13}$$

where ω is an inertia factor that controls the iterative velocity of particles, V_k is the velocity of the particle in the last iteration, V_{k+1} is the velocity after this update. P_i is the individual extremum and P_g is population extremum. c_1 and c_2 are non-negative constants. r_1 and r_2 are random numbers between 0 and 1. X_k is the position of particle before updated, $X_k + 1$ is the position of particle after updated.

(c) Repeat the calculation process of the second step until all particles converge to a certain point. The optimal particle of the population can be mapped as the optimal value of the penalty parameter c and kernel function parameter g.

TABLE 2. Arc fault detection accuracy of SVM, BP and PSO-SVM.

Load	Samples number	Correct number			Correct rate		
		SVM	BP	PSO-SVM	SVM	BP	PSO-SVM
Incandescent lamp and inductor in series	40	37	37	40	92.5%	92.5%	100%
Incandescent lamp	40	35	15	40	87.5%	37.5%	100%
Electric drill	40	31	23	38	77.5%	57.5%	95%
Computer	40	29	30	35	72.5%	75%	87.5%
Induction cooker	40	28	34	38	70%	85%	95%
Total	200	160	139	191	80%	69.5%	95.5%

The arc fault is detected by PSO-SVM. The evolutionary algebra of PSO is set to 200, the population size is 40, the maximum and minimum values of the parameter c are 100 and 0.1 respectively, the maximum and minimum values of the parameter g are 1000 and 0.1 respectively. Forty groups of data are taken as testing samples each type of load circuit. Then the total of training samples is two hundred groups of data.

The parameter optimization process of incandescent lamp and inductor in series load circuit is taken as an example, as shown in Figure 13. It shows the changes of the optimal fitness value and the average fitness value in the iterative process of the PSO algorithm. The horizontal axis is the number of training steps and the vertical axis is the fitness value. The parameter c is equal to 0.675, and g is equal to 13.36.

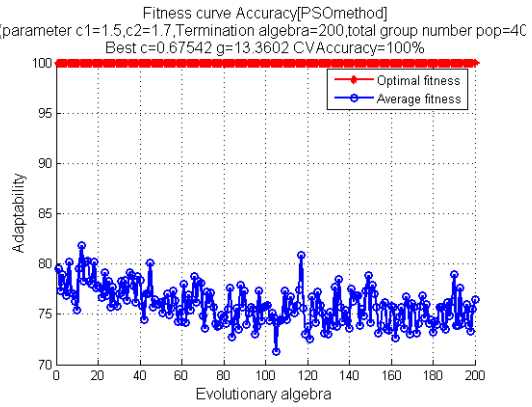

FIGURE 13. PSO iteration process (incandescent lamp and inductor in series).

The arc fault detection results are carried out through PSO-SVM,conventional SVM and BP network respectively, as shown in Table 2. The detection result of computer load circuit is shown as a representative in Figure 14. The horizontal axis represents the sample number, and the vertical axis represents the work state, *i.e.* 1 represents normal work and 2 represents arc fault. The blue circle indicates the actual work state and the red asterisk indicates the detection result of network. If the two symbols coincide, the result is right. Otherwise, the result is wrong. As can be seen from Figure 14 and Table 2, the detection accuracy of PSO-SVM model is 95.5% and it is much higher than 80% of SVM model and 69.5% of BP model. Among them, the accuracy of PSO-SVM model is 100% when the loads are incandescent lamp and inductor in series and incandescent lamp.

V. DISCUSSION

A. CURRENT CHARACTERISTICS

The normal current waveforms and arc fault current waveforms has different characteristics under different types of loads conditions. The current waveform of arc fault has ''zero rest'' characteristic under the condition of incandescent lamp load, electric drill load and induction cooker load. When the load is a computer, the normal current waveform also appears ''zero rest'' characteristic. The current waveform of computer load in normal work is similar to that of incandescent lamp load in arc fault.

B. CURRENT FEATURE EXTRACTION

The current features are extracted in time domain and frequency domain, so that the current characteristics can be better reflected. Four features of current in time domain are current average, current pole difference, difference current average and current variance. The current average can represent the overall distribution of current value in time domain and reduce the influence of individual abnormal current value. The current pole difference can reflect the change of current value in a certain time segment. The difference current average can reflect the change of current value in adjacent two time segments. The current variance represents the dispersion of current amplitude in each time segment. These four features can reflect the time domain characteristics of current more completely. The current amplitude spectrum is obtained by FFT, and the frequency range is 0-2000 Hz. AC frequency is 50 Hz and forty current amplitudes are obtained. The frequency range of 0-2000 Hz is divided into ten equal length segments, then forty amplitudes are also divided into ten groups, i.e. four amplitudes in each group. There are two reasons for calculating the average of four current amplitudes. 1) The average value can reflect the amplitude characteristics of each segment of data. 2) The average value in each frequency segment replaces all the original data, which can reduce the dimension of the network input samples and the computations.

C. THE LIMITATION OF THE PROPOSED METHOD

This study mainly focuses on arc fault detection of single load circuit and is the preliminary to a more complete development. The proposed method is not suitable for arc fault

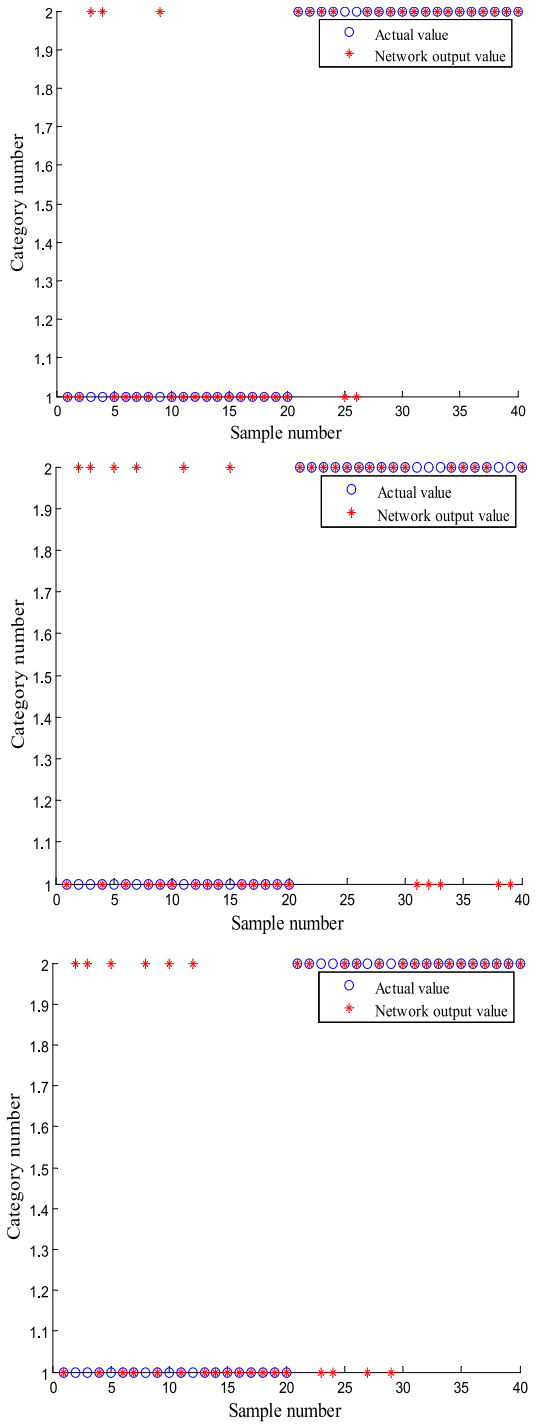

FIGURE 14. Detection results of computer load circuit. (a) PSO-SVM model. (b) SVM model. (c) BP network model.

detection in multi-load circuit. Arc fault detection of multi-load circuit is our next job.

VI. CONCLUSION

In this paper, the arc fault experimental platform is used to collect circuit current data under five load types conditions and the current features of time domain and frequency domain are extracted. Thirty-nine numbers are extracted from four features of current in time domain. Ten average amplitudes are extracted as frequency domain feature. These forty-nine numbers can more fully reflect the current characteristics of normal work and arc fault.

The proposed method can not only detect arc fault, but also determine which type of load circuit produces fault. The load type identification belongs to the multi-classification problem. The LVQ-NN structure is suitable for multi-classification problems and can be used to judge different types of loads. It can reflect the influence of arc fault on current in different types of load circuits. The problem of arc fault detection belongs to the two-classification (normal work or arc fault) problem, so the SVM with good performance of the two-classification is a better choice. The classification performance of SVM greatly depends on appropriate selection of parameters c and g. In order to improve the calculation speed and classification accuracy, PSO algorithm is used to optimize c and g. PSO-SVM has higher accuracy in arc fault detection, compared with BP neural network and conventional SVM.

REFERENCES

[1] J. L. Guardado, S. G. Maximov, E. Melgoza, J. L. Naredo, and P. Moreno, "An improved arc model before current zero based on the combined Mayr and Cassie arc models," *IEEE Trans. Power Del.*, vol. 20, no. 1, pp. 138–142, Jan. 2005.

[2] A. Khakpour, S. Franke, S. Gortschakow, D. Uhrlandt, R. Methling, and K.-D. Weltmann, "An improved arc model based on the arc diameter," *IEEE Trans. Power Del.*, vol. 31, no. 3, pp. 1335–1341, Jun. 2016.

[3] U. Habedank, "Application of a new arc model for the evaluation of short-circuit breaking tests," *IEEE Trans. Power Del.*, vol. 8, no. 4, pp. 1921–1925, Oct. 1993.

[4] K. Qiao, W. Z. Liu, and J. Zhang, "Simulation of off-line arc simulation of bow network based on improved Mayr mode," *Railway Standard Des.*, vol. 62, no. 5, pp. 138–142, 2018.

[5] P. H. Schavemaker and L. van der Slui, "An improved Mayr-type arc model based on current-zero measurements," *IEEE Trans. Power Del.*, vol. 15, no. 2, pp. 580–584, Apr. 2000.

[6] R. Hu, "Research on the influence of different arc models on circuits," *Northeast Electr. Power Technol.*, vol. 39, no. 5, pp. 18–20, 2018.

[7] Q. Wang, Z. Ye, and W. J. Tan, "Simulation and analysis of precise breakdown arc model," *Power Syst. Clean Energy*, vol. 31, no. 10, pp. 4–9, 2015.

[8] T. Yan, W. H. Wu, and C. H. Xu, "Calculation and analysis of VFTO under trapezoidal dynamic arc model," *Electr. Porcelain Arrester*, vol. 4, no. 12, pp. 188–193, 2018.

[9] Q. L. Wang, B. W. Wang, and H. L. Guan, "Model and experiment of low voltage AC series fault arc," *J. Electr. Power Syst. Autom.*, vol. 30, no. 2, pp. 26–30, 2018.

[10] N. Qu, J. H. Wang, and J. H. Liu, "An arc fault detection method based on multidictionary learning," *Math. Problems Eng.*, vol. 2018, pp. 1–8, Dec. 2018.

[11] L. Kumpulainen, G. A. Hussain, M. Lehtonen, and J. A. Kay, "Preemptive arc fault detection techniques in switchgear and controlgear," *IEEE Trans. Ind. Appl.*, vol. 49, no. 4, pp. 1911–1919, Jul./Aug. 2013.

[12] P. Qi, S. Jovanovic, J. Lezama, and P. Schweitzer, "Discrete wavelet transform optimal parameters estimation for arc fault detection in low-voltage residential power networks," *Electr. Power Syst. Res.*, vol. 143, pp. 130–139, Feb. 2017.

[13] R. Grassetti, R. Ottoboni, M. Rossi, and S. Toscani, "Low cost arc fault detection in aerospace applications," *IEEE Instrum. Meas. Mag.*, vol. 16, no. 5, pp. 37–42, Oct. 2013.

[14] J. K. Zhang, Q. L. Deng, and J. C. Tang, "Characteristic analysis and modeling of series fault arc," *Electr. Eng.*, vol. 1, pp. 30–32, Jan. 2017.

[15] K. Koziy, B. Gou, and J. Aslakson, "A low-cost power-quality meter with series arc-fault detection capability for smart grid," *IEEE Trans. Power Del.*, vol. 28, no. 3, pp. 1584–1591, Jul. 2013.
[16] Q. F. Yu, "Electrical fire prediction system based on wavelet analysis and data fusion and its application," M.S. thesis, Yanshan Univ., Qinhuangdao, China, May 2013.
[17] G. Artale, A. Cataliotti, V. Cosentino, D. Di Cara, S. Nuccio, and G. Tinè, "Arc fault detection method based on CZT low-frequency harmonic current analysis," *IEEE Trans. Instrum. Meas.*, vol. 66, no. 5, pp. 888–896, May 2017.
[18] I. Baqui, I. Zamora, J. Mazón, and G. Buigues, "High impedance fault detection methodology using wavelet transform and artificial neural networks," *Electr. Power Syst. Res.*, vol. 81, no. 7, pp. 1325–1333, Jul. 2011.
[19] Z. J. Wang, F. Zhang, and S. W. Zhang, "Research on low voltage series fault arc recognition method based on support vector machine," *Electr. Meas. Instrum.*, vol. 50, no. 4, pp. 22–26, 2013.
[20] S. H. Mortazavi, Z. Moravej, and S. M. Shahrtash, "A hybrid method for arcing faults detection in large distribution networks," *Int. J. Elect. Power Energy Syst.*, vol. 94, pp. 141–150, Jan. 2018.
[21] A. Yaramasu, Y. Cao, G. Liu, and B. Wu, "Aircraft electric system intermittent arc fault detection and location," *IEEE Trans. Aerosp. Electron. Syst.*, vol. 51, no. 1, pp. 40–51, Jan. 2015.
[22] N. L. Georgijevic, M. V. Jankovic, S. Srdic, and Z. Radakovic, "The detection of series arc fault in photovoltaic systems based on the arc current entropy," *IEEE Trans. Power Electron.*, vol. 31, no. 8, pp. 5917–5930, Aug. 2016.
[23] N. Qu, J. Wang, and J. Liu, "An arc fault detection method based on current amplitude spectrum and sparse representation," *IEEE Trans. Instrum. Meas.*, vol. 68, no. 10, pp. 3785–3792, Oct. 2019.
[24] C. Y. Zhang, "Analysis of electrical fire intelligent algorithm based on arc model simulation," M.S. thesis, Zhejiang Univ., Hangzhou, China, Jan. 2016.
[25] X. K. Guo, T. Jian, and Y. L. Dong, "Radar one-dimensional range image recognition based on PSO-KPCA-LVQ neural network," *Electro-Opt. Control*, vol. 26, no. 6, pp. 22–26, 2019.
[26] Z. B. Wang, H. W. Cao, and J. J. Liu, "Research on fault arc detection algorithm based on wavelet packet denoising and EMD," *Electr. Meas. Instrum.*, vol. 56, no. 6, pp. 118–121, 2019.
[27] Z. H. Xu, "Low-voltage fault arc identification method based on support vector machine," *J. Electr. Power Syst. Autom.*, vol. 24, no. 2, pp. 128–131, 2012.

NA QU received the M.S. degree in power electronics and transmission from Northeastern University, Shenyang, China, in 2005, where she is currently pursuing the Ph.D. degree. She is currently an Associate Professor with Shenyang Aerospace University.

She has published more than 20 articles in major journals and international conferences. Her current research interests include arc fault and electrical fire detection, and intelligent information processing.

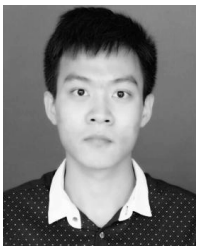

JIANKAI ZUO is currently pursuing the dual B.S. degrees in network engineering with the School of Computer Science, Shenyang Aerospace University, Shenyang, China, and in business administration from Northeastern University.

Due to his excellent academic performance and strong scientific research ability, he was promoted in computer science and technology with Tongji University, Shanghai (directly study for a Ph.D. degree). He has published more than eight articles in journals and international conferences. His research interests include machine learning, deep learning, pattern recognition, and computer vision.

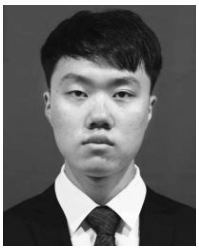

JIATONG CHEN is currently pursuing the B.S. degree in energy and power engineering from Shenyang Aerospace University, Shenyang, China.

He has published more than five articles in journals and international conferences. His research interests include intelligent information processing, deep learning, and data mining.

ZHONGZHI LI is currently pursuing the B.S. degree in computer science and technology from Shenyang Aerospace University, Shenyang, China.

His research interests include machine learning, deep learning, computer vision, few shot learning, and domain adaptation.